Title

Mutational and secondary structural analysis of the basolateral sorting signal of the polymeric immunoglobulin receptor.

Journal

Journal of Cell Biology, 123(5)

ISSN

0021-9525

Authors

Aroeti, B
Kosen, PA
Kuntz, ID
et al.

Publication Date

1993-12-01

DOI

10.1083/jcb.123.5.1149

Peer reviewed

Mutational and Secondary Structural Analysis of the Basolateral Sorting Signal of the Polymeric Immunoglobulin Receptor

Benjamin Aroeti,*‡¶ Phyllis A. Kosen,§ Irwin D. Kuntz,‡§ Fred E. Cohen,§‡‖ and Keith E. Mostov*‡¶

Departments of *Anatomy, ‡Biochemistry and Biophysics, §Pharmaceutical Chemistry, and ‖Medicine, and ¶Cardiovascular Research Institute, University of California, San Francisco, California 94143

Abstract. The 17-juxtamembrane cytoplasmic residues of the polymeric immunoglobulin receptor contain an autonomous basolateral targeting signal that does not mediate rapid endocytosis (Casanova, J. E., G. Apodaca, and K. E. Mostov. *Cell.* 66:65–75). Alanine-scanning mutagenesis identifies three residues in this region, His656, Arg657, and Val660, that are most essential for basolateral sorting and two residues, Arg655 and Tyr668, that play a lesser role in this process. Progressive truncations suggested that Ser664 and Ile665 might also play a role in basolateral sorting. However, mutation of these residues to Ala or internal deletions of these residues did not affect basolateral sorting, indicating that these residues are probably not required for basolateral sorting. Two-dimensional NMR spectroscopy of a peptide corresponding to the 17-mer signal indicates that the sequence Arg658-Asn-Val-Asp661 has a propensity to adopt a β-turn in solution. Residues COOH-terminal to the β-turn (Arg662 to Arg669) seem to take up a nascent helix structure in solution. Substitution of Val660 with Ala destabilizes the turn, while mutation of Arg657 to Ala does not appear to affect the turn structure. Neither mutation detectably altered the stability of the nascent helix in the COOH-terminal portion of the peptide.

POLARIZED epithelial cells have two plasma membrane domains: the apical domain facing the external environment, and the basolateral domain facing the internal milieu. These domains display striking differences in protein and lipid composition (Caplan and Matlin, 1989; Simons and Wandinger-Ness, 1990; Rodriguez-Boulan and Nelson, 1989; Gumbiner, 1990; Nelson, 1992; Mostov et al., 1992; Rodriguez-Boulan and Powell, 1992). In MDCK cells, most newly made plasma membrane proteins are directly targeted from the TGN to either the apical or basolateral surface (Rodriguez-Boulan and Nelson, 1989; Simons and Wandinger-Ness, 1990; Le Bivic et al., 1990; Lisanti and Rodriguez-Boulan, 1990). Until recently, it had been presumed that targeting to the apical cell surface is a signal-mediated process, whereas targeting to the basolateral surface occurs by "default" (Simons and Wandinger-Ness, 1990; Bomsel and Mostov, 1991). However, studies using wild-type and mutant forms of plasma membrane proteins (examples: low-density lipoprotein receptor [LDLR][1], lysosomal protein lgp120, Fc receptor [FcR-II], lysosomal acid phosphatase [LAP], and polymeric immunoglobulin receptor [pIgR]) expressed in MDCK cells showed that the cytoplasmic domain of these proteins contain active sorting signals mediating targeting from the TGN to the basolateral surface (Hunziker et al., 1991; Casanova et al., 1991; Mostov et al., 1992). When mutations in the cytoplasmic tail inhibited basolateral targeting, the proteins were instead delivered to the apical plasma membrane.

The basolateral sorting signals so far analyzed can be placed into two categories. Most of the signals appear to be colinear with Tyr-containing signals for endocytosis via clathrin-coated pits (Hunziker et al., 1991; Brewer and Roth, 1991; Le Bivic et al., 1991; reviewed in Mostov et al., 1992). In several other cases (e.g., the transferrin receptor and vesicular stomatitis virus G protein) basolateral sorting signals appear not to overlap with endocytosis signals (Hunziker et al., 1991; Dargemont et al., 1993; Thomas et al., 1993). The cytoplasmic domain of the LDLR contains two basolateral signals, one of each type. The membrane proximal basolateral signal is colinear with the signal for endocytosis, while the membrane distal signal does not overlap with an endocytosis signal (Matter et al., 1993).

For those basolateral signals that are colinear with coated-pit internalization motifs, it has been suggested that both signals may share common structural features (Mostov et al., 1992). The three-dimensional structure of the tyrosine-containing endocytosis signal of the transferrin receptor was predicted by computer modeling to be a type I β-turn (Col-

Address all correspondence to Dr. B. Aroeti, Department of Anatomy, Box 0452, University of California, San Francisco, CA 94143-0452.

1. *Abbreviations used in this paper*: HOHAHA, homonuclear Hartmann-Hahn; LAP, lysosomal acid phosphatase; LDLR, low-density lipoprotein receptor; NOE, nuclear Overhauser effects; pIgR, polymeric immunoglobulin; SC, secretory component; TfR, transferrin receptor; 2D-NMR, two dimensional nuclear magnetic resonance.

lawn et al., 1990). Subsequent structure determinations by two-dimensional nuclear magnetic resonance (2D-NMR) spectroscopy showed that synthetic peptides corresponding to the endocytosis signals of LDLR, LAP, and insulin receptor probably adopt a type I β-turn conformation in solution (Bansal and Gierasch, 1991; Eberle et al., 1991; Lehmann et al., 1992; Backer et al., 1992; reviewed in Vaux, 1992).

The 19-amino acid cytoplasmic domain of LAP that specifies both basolateral sorting and endocytosis has been particularly well studied. Mutation of Tyr413 to Phe blocks endocytosis in MDCK cells, but not TGN to basolateral targeting, suggesting that the two types of signals can be separated (Prill et al., 1993). Analysis of the corresponding peptide by NMR indicates that this mutation destabilizes the β-turn by about 25% (Lehmann et al., 1992). Mutation of Tyr413 to Ala blocks both endocytosis and basolateral sorting, and NMR analysis shows that the β-turn is destabilized by about 50% (Lehmann et al., 1992). These data suggest that for those basolateral signals that overlap with endocytosis signals, a β-turn is an important part of both signals. However, the precise requirements for basolateral signals and endocytosis signals appear to differ.

We have limited information on the sequence requirements for basolateral signals that do not overlap with endocytosis signals. In the case of the membrane-distal LDLR basolateral signal, Tyr 35 as well as Tyr 37 seem to be required for basolateral sorting (Matter et al., 1992). Furthermore, we have no information on the three-dimensional structure of such signals.

Targeting of the pIgR from the TGN to the basolateral surface is mediated by a signal localized in the plasma membrane proximal 17 amino acids (residues 653–669) of the 103 residues comprising the COOH-terminal cytoplasmic domain (Casanova et al., 1991). A deletion of 14 residues (655–668) in the 17-mer segment that leaves the remaining COOH-terminal 89-amino acids of the cytoplasmic domain fused in frame to the transmembrane region, causes a substantial loss of basal targeting. The mutant receptor is delivered instead to the apical surface. Most importantly, transfer of the 17-mer sequence to an apical protein, placental alkaline phosphatase, redirects it to the basolateral surface. This experiment demonstrates that the 17-mer sequence is sufficient to cause sorting from the Golgi apparatus to the basolateral surface in a dominant and autonomous manner.

The pIgR basolateral signal acts independently of endocytosis. The cytoplasmic domain of the pIgR contains two tyrosines (Tyr668 and Tyr734) which are involved in endocytosis (Okamoto et al., 1992). Mutation of Tyr734 (which resides near the COOH-terminal portion of the molecule) to a Ser severely blocks endocytosis, whereas mutation of Tyr668 to a Cys has a minor effect. Mutation of either one or both tyrosines inhibits endocytosis but not basolateral delivery (Okamoto et al., 1992), suggesting that residues other than tyrosines can mediate basolateral sorting of the pIgR. The 17-residue basolateral targeting signal of the pIgR contains Tyr668 as its penultimate residue. The truncated pIgR containing only the 17-residue segment is efficiently targeted to the basolateral surface but not endocytosed (Casanova et al., 1991). Interestingly, the mutant pIgR that lacks 14 amino acids of the 17-residue signal but contains the rest of the cytoplasmic domain is apically targeted and efficiently endocytosed, as it retains Tyr734 (Casanova et al., 1991).

The pIgR basolateral sorting signal is one of the best defined examples of a basolateral signal that is independent of endocytosis. As little is known about the sequence requirements and structural features of such signals, we performed a detailed mutational analysis of the 17-residue signal in order to identify individual amino acids that might play an important role in basolateral targeting of the pIgR. We used several strategies, including progressive truncations from the COOH terminus, alanine scanning mutagenesis, and internal deletions. By using high-resolution two-dimensional ^{1}H NMR spectroscopy we also assessed the nature of potential structural elements in a synthetic 17-mer peptide corresponding to this signal.

Materials and Methods

Generation of Cell Lines Expressing Mutant pIgRs

All mutants were generated by oligonucleotide site-directed mutagenesis according to the method of Kunkel (Kunkel, 1985). The cDNA encoding the pIgR was subcloned into the vector M13mp8 as described previously (Mostov et al., 1986). Unless otherwise mentioned, mutations were constructed using a mutant DNA generated by insertion of a stop codon instead of T670 as a starting template. In frame deletion of amino acids 656–658 was performed using a mutagenic oligonucleotide that was complementary to nucleotides 2131–2142 5′ to the deletion site and nucleotides 2152–2163 3′ to the deleted segment. In frame deletions of Ser664 or Ile665 were performed in the context of the full-length pIgR. For deleting Ser664 we used an oligonucleotide complementary to nucleotides 2155–2166 and 2170–2182 of the pIgR cDNA. An oligonucleotide complementary to nucleotides 2158–2169 and 2173–2185 was used to delete Ile665. The mutagenic oligonucleotide (5′-CGG CAC AGG AGG GAC AAC CGA GTA GTT TCC ATC GGA-3′) was used to scramble the order of the sequence NVDR (659–661) to DNRV (the nucleotides encoding the DNRV residues are underlined). The sequences of primers used for truncation of residues (i.e., mutating the relevant codon to a stop codon) and alanine substitutions are available on request. The mutagenized sequences were confirmed by dideoxy sequencing using the Sequenase kit (United States Biochemical Corp., Cleveland, OH). For the expression of mutants, the replicative form phage DNA was isolated and the cDNA fragment was prepared by endonuclease BglII digestion and agarose gel electrophoresis. The isolated cDNA fragment was then ligated into the BglII sites of the cytomegalovirus promoter-based expression vector, pCB6 (Brewer and Roth, 1991), using standard techniques (Maniatis et al., 1982).

MDCK strain II cells were transfected by calcium phosphate precipitation, followed by selection with G418 sulfate (GIBCO-BRL, Gaithersburg, MD) (0.7 mg/ml in growth medium for 14–18 d). Individual clones were isolated with glass cylinders, grown to confluence in plastic dishes, and tested for pIgR expression by metabolic labeling and immunoprecipitation as described previously (Breitfeld et al., 1989*b*). The polarity of all clones was determined by methionine uptake and secretion of an endogenous glycoprotein complex (Urban et al., 1987; Casanova et al., 1991; Okamoto et al., 1992). All cell lines were assessed to be similarly polarized. Additionally, to obtain a population of pooled clones, ~50–200 clones on a single 10-cm dish were grown to confluence. All experiments were performed using cell lines of passage number 2 through 15 after cloning.

Cell Culture

MDCK (strain II) cells were grown in MEM (CellGro; Mediatech, Washington, D.C.) supplemented with 5% FBS (HyClone, Logan, UT), 100 U/ml penicillin, 100 U/ml streptomycin, and 0.25 μg/ml Fungizone in 5% CO_2, 95% air. In all cases, cells (~2×10^6 cells/ml) were cultured on Transwell polycarbonate filter units (0.4-μm pore size; 24-mm diam; Costar Corp., Cambridge, MA) for 4–5 d before the experiments (Breitfeld et al., 1989*b*). Fresh medium was added every other day after plating onto filters.

Vectorial Delivery of the pIgR

Normally the pIgR is delivered directly from the TGN to the basolateral surface. The pIgR is then endocytosed and sorted into transcytotic vesicles that carry it to the apical surface (Brietfeld et al., 1989*a*). After reaching the apical surface an endogenous protease cleaves the extracellular, ligand

binding domain and releases this domain into the apical medium. This cleaved fragment is called secretory component (SC). With the wild-type pIgR ~15% of the molecules leaving the TGN do not reach the basolateral surface, but instead are targeted directly to the apical surface and then cleaved to SC. The basic principles of the protease sensitivity assay for vectorial delivery of newly synthesized pIgR to the basolateral surface were described earlier (Casanova et al., 1991). We have modified the assay to obtain more accurate and quantitative data (Apodaca et al., 1993). A pair of filters containing confluent monolayer of MDCK cells were used for each determination. Cells were starved in MEM lacking cysteine (obtained from UCSF Cell Culture Facility; supplemented with 5% dialyzed FBS) for 15 min at 37°C. Then, the cells were pulse-labeled for 15 min at 37°C in starvation medium supplemented with [^{35}S]cysteine (1,130 Ci/mmol, 10.5 mCi/ml; New England Nuclear, Boston, MA), to a final concentration of 1.75 μCi/μl, and washed three times quickly with warm MEM-BSA (MEM containing Hank's balanced salts, 20 mM Hepes, pH 7.3, antibiotics, and 0.6% BSA). Both filters were chased for 90 min at 37°C, to allow the cohort of labeled receptors to reach the cell surface. The first filter, which served as control, was chased in the presence of MEM-BSA (1 ml in the apical and basolateral compartments). The second filter was chased in the continuous presence of MEM-BSA supplemented with V8 protease (25 μg/ml; Boehringer-Mannheim Biochemicals, Indianapolis, IN) at the basolateral compartment, and MEM-BSA without added protease in the apical compartment. The administration of V8 protease yielded more consistent and accurate results than the previously used TPCK-trypsin. At the end of the chase period, both the apical and basal media of the first (control) filter and the apical medium of the protease-treated filter were harvested and SC was immunoprecipitated as described below. Filters were washed three times with ice-cold MEM-BSA containing 10% FBS, excised, and subjected immediately to immunoprecipitation as below. For all mutants described here we performed 10–13 analyses, each of which consisted of a control filter and a V8-treated filter.

Immunoprecipitation

Cells on filters were boiled for 5 min in 1 ml of 0.5% SDS lysis buffer (0.5% SDS, 150 mM NaCl, 5 mM EDTA, 100 U/ml Trasylol, 20 mM Triethanolamine-HCl, pH 8.1), and vortexed vigorously for 15 min. Basal and apical media were transferred to a microfuge tube containing 80 μl of 10% SDS, and boiled for 5 min. Triton dilution buffer (0.5 ml, 5% Triton X-100, 100 mM NaCl, 5 mM EDTA, 100 U/ml Trasylol, 0.1% NaN_3, 2 mM PMSF, 50 mM triethanolamine-HCl, pH 8.6) was then added to each sample. Samples were pre-cleared twice with Sepharose CL-2B (Breitfeld et al., 1989*b*), and pIgR molecules were immunoprecipitated by overnight incubation (4°C; continuous end-over-end rotation) with 30 μl of protein G-Sepharose (15% slurry; Sigma Immunochemicals, St. Louis, MO) to which polyclonal sheep anti-SC IgG had been covalently coupled using 20 mM dimethylpimelimidate (Gersten and Marchalonis, 1978). Beads were washed three times with "mixed micelle buffer" (1% Triton X-100, 0.2% SDS, 150 mM NaCl, 5 mM EDTA, 8% sucrose, 0.1% NaN_3, 10 U/ml Trasylol, and 20 mM triethanolamine-HCl, pH 8.6) followed by one wash with "final wash" buffer (i.e., mixed micelle buffer lacking detergent) and prepared for SDS-PAGE as described (Brietfeld et al., 1989*b*; Casanova et al., 1991).

Quantitative Analysis of Vectorial Delivery

Fig. 2 depicts a typical delivery assay performed on the T670-stop mutant receptor. The radioactivity levels of bands corresponding to pIgR and SC immunoprecipitated from cells and media, respectively, were determined by a PhosphorImager (Molecular Dynamics, Sunnyvale, CA). The total amount of radiolabeled pIgR immunoprecipitated from V8 non-treated cells ($TpIgR^{V8-}$) over the 90-min chase at 37°C was determined: $TpIgR^{V8-} = pIgR^{V8-} + [A]SC^{V8-} + [B]SC^{V8-}$, where $pIgR^{V8-}$ is the radioactivity level measured for pIgR immunoprecipitated from V8 non-treated cells, and $[A]SC^{V8-}$ and $[B]SC^{V8-}$ are radioactivity levels measured for SC immunoprecipitated from the acpial and basolateral media of the same cells, respectively. The amount of radiolabeled pIgR in cells detected under equivalent experimental conditions but in the continuous presence of V8 protease at the basolateral medium is reduced (compare label intensities of bands $pIgR^{V8+}$ and $pIgR^{V8-}$ in lanes *2* and *1*, respectively). This reduction is due to V8-mediated proteolysis of newly synthesized pIgR delivered to the basolateral plasma membrane in the course of the 90-min chase. The amount of basolaterally delivered receptor is derived from the reduction in radiolabel signal contributed by pIgR in V8-treated cells. Thus, the total amount of radiolabeled pIgR in V8-treated cells ($TpIgR^{V8+}$) is: $TpIgR^{V8+} = pIgR^{V8+} + [A]SC^{V8+}$. The population (in percentage) of newly synthesized receptors delivered to the basolateral surface was determined as follows:

$$\text{Basolateral Delivery (\%)} = (1 - TpIgR^{V8+}/TpIgR^{V8-}) \times 100.$$

SC comprises the major portion of the extracellular ligand-binding domain of the receptor and it contains all but one of the cysteine residues labeled with ^{35}S. Once pIgR molecules arrive at the apical surface they are efficiently cleaved by an endogenous protease to SC which is released into the apical medium (Casanova et al., 1991). This is in contrast to the basolateral endogenous protease which acts inefficiently, releasing small amounts (<5% of the total label; see Fig. 2, lane *5*) of SC to the basal medium. The high efficiency of pIgR cleavage at the apical surface was confirmed in control experiments in which V8 protease was included in the apical medium during the entire chase period. In all cases, the apically added V8 had no effect on the amount of pIgR immunoprecipitated from cells (compare the intensities of pIgR bands in lanes *1* and *3* in Fig. 2), indicating that there was not a substantial pool of pIgR that had reached the apical surface and had not been cleaved to SC. Apical SC can in principle have two sources: pIgR delivered directly from the TGN to the apical surface and pIgR that was first delivered to the basolateral surface and then transported to the apical surface via transcytosis. However, direct apical targeting was assessed by measuring the amount of apically released SC in the presence of basolateral V8 (band $[A]SC^{V8+}$ in lane *6*) which effectively eliminated the population of transcytosing pIgRs. Therefore, the fraction of pIgR delivered from the TGN to the apical plasma membrane was calculated as follows:

$$\text{Apical Delivery (\%)} = ([A]SC^{V8+}/TpIgR^{V8-}) \times 100.$$

In experiments performed on mutant receptors in the context of the truncated T670-stop receptor, the average amount (of many experiments) of SC immunoprecipitated from the apical medium of V8 non-treated cells was roughly comparable to that released into the apical medium of V8-treated cells. This can be directly attributed to the fact that all pIgR mutants were severely blocked in endocytosis and subsequent transcytosis. The fact that V8 treatment largely did not affect direct apical delivery of pIgR also suggests that V8 had no general effects on receptor traffic from the Golgi apparatus to the plasma membrane, and that V8 does not cross the tight cell monolayer from the basolateral to the apical compartment. The latter notion is also favored by the following two observations. First, the *trans*-monolayer electrical resistance of monolayers treated with basolateral protease (trypsin or V8) was not significantly different from non-protease-treated monolayers (data not shown), implying that the tight junctions are intact and maintain their barrier activity in the presence of the protease. Second, if either basolateral or apical medium that contained protease is subjected to immunoprecipitation (at the end of the 90-min chase and after boiling with SDS to inactivate the protease) with anti-SC antibodies, a ladder of bands with molecular weights smaller than that of SC is observed. These bands presumably represent degradation products of receptors that arrived at the cell surface during the chase and were cleaved by the V8 protease. In experiments where V8 was added to the basolateral medium, if the protease had leaked into the apical medium and cleaved pIgR at the apical surface (or cleaved SC in the apical medium) we would have expected to find this ladder in the immunoprecipitates from the apical medium. However, in all experiments where SC was immunoprecipitated from the apical medium of monolayers that were treated with basolateral protease, neither this ladder nor any other bands except for SC were ever observed, suggesting that such leakage did not occur.

The advantage of this protease-based delivery assay over surface biotinylation-based assays is that it directly measures the integrated amount of pIgR inserted into the basolateral and apical plasma membranes over the entire chase period. Conceivably, rapid endocytosis and transcytosis may enable receptor to avoid the exogenous protease, a phenomenon which might lead to inaccurate determination of basolateral delivery. However, as indicated above, all mutants were severely blocked in endocytosis (but not basolateral delivery), causing receptor accumulation on the basolateral cell surface and its continual exposure to the V8 protease.

Peptide Synthesis

Peptides representing the wild-type 17-mer basolateral targeting signal of pIgR (residues 653-669; see Fig. 1 *a*), and the two mutant signals were synthesized on a Milligen/Bioresearch 9050 automated peptide synthesizer, using FMOC synthetic chemistry (Stanford University Medical Center, Protein and Nucleic Acid Facility, Beckman Center). All peptides synthesized were purified by preparative reverse-phase high pressure liquid chromatography (preparative column was a Millipore 25 mm × 10 cm C_{18}

RCM; Millipore Corp., Bedford, MA) and analyzed by amino acid analysis and mass spectroscopy.

2D NMR

Proton NMR spectra were acquired using a spectrometer (GN-500; General Electric Co., Wilmington, MA). Experiments were run in the phase-sensitive mode with quadrature detection in both dimensions. Spectral widths were 6,024 Hz. All data processing and analysis were performed using software developed for a Sun work station by M. Day and D. Kneller in the laboratory of I. D. Kuntz (University of California, San Francisco, CA). Base-line correction has been described (Basus, 1984). Sample concentrations were approximately 7–9 mM in 10% D_2O/90% H_2O and included 1 mM sodium (trimethylsilyl)-propionate (TSP) as an internal reference. Sample pH was adjusted to 4.6, without correction for the deuterium isotope effect, by addition of small amounts of NaOH and HCl.

For homonuclear Hartmann-Hahn (HOHAHA) spectra with MLEV-17 (Bax et al., 1982) the spectrometer was modified by inclusion of a 6-W amplifier as the transmitter with a γH_1 of 8 kHz as described (Basus et al., 1988). A 75-ms mixing time was used. The H_2O signal was suppressed with the DANTE sequence (Morris and Freeman, 1978). This period (4 s) incorporated the recycle time. The number of t_1 increments was 512, each with four acquisitions and 4,096 data points in t_2. One dummy scan was performed prior to each t_1 increment. The data, in both dimensions, were modified by a Gaussian function with a line broadening component of −1.5 Hz and a multiplier of 0.11. The spectra were zero-filled once in each domain.

The temperature coefficients of the amide chemical shifts for P-WT and P-660A were determined from HOHAHA spectra acquired at 2, 5, 10, 15, 20, 25, 30, and 35 or 40°C.

Nuclear Overhauser effect (NOESY) spectra were acquired at 5°C using the procedure of States et al. (States et al., 1982). A 200-ms mixing time was used. The H_2O resonance was selectively removed by use of a jump-and-return read pulse, plus a short (3 ms) pulsed field gradient at the start of the mixing period (Basus, 1984; Plateau and Guéron, 1982). A recycle time of 2.5 s was used. Spectra were acquired with 1,024t_1 increments, each with 16 acquisitions and 4,096 data points in t_2. One dummy scan was performed before each increment. The data were multiplied with a squared sine-bell function shifted 50° in t_2 and 80° in t_1. The spectra were zero filled once in the t_1 domain and twice in the t_2 domain.

Results

Identification of Specific Residues That Comprise the Basolateral Sorting Signal of the pIgR

To identify specific residues required for basolateral sorting, we systematically mutated the 17-residue basolateral sorting signal in the cytoplasmic domain of the pIgR. The mutagenesis strategies and designation of each mutant receptor are summarized in Fig. 1. Mutant cDNAs were transfected into MDCK cells, and cell lines stably expressing mutant receptors were generated. All amino acid substitutions and most other mutations were constructed in the background of the mutant receptor T670-stop (i.e., the codon for T670 is replaced by a stop codon), which truncates the cytoplasmic domain at residue 669. Since the 17-residue cytoplasmic segment contains the information required for efficient basolateral targeting, we used the T670-stop template as a simplifying model to dissect the basolateral sorting signal. Moreover, we employed this strategy to eliminate possible contributions from signals that might exist COOH-terminal to the 17-mer segment, between residues 670 and 755.

Vectorial delivery of each mutant receptor from the TGN to the basolateral surface was quantitatively determined by combining a pulse-chase procedure with protease treatment (Apodaca et al., 1993) as detailed in Materials and Methods and Fig. 2. MDCK cells expressing mutant pIgRs were grown on polycarbonate Transwell filters. Receptors were metabolically labeled for 15 min with [^{35}S]Cys, and delivery of these newly synthesized (radiolabeled) receptors to the cell surface was followed over a 90-min chase period. The radiolabeled receptors were either chased in plain medium (control cells) or chased in the presence of V8 protease in the medium bathing the basolateral surface. In the latter case, pIgR molecules delivered from the TGN to the basolateral surface were proteolyzed and could not be immunoprecipitated as full length pIgR. Consequently, a reduction in radiolabeled receptor was observed (Fig. 2), reflecting the integrated amount of receptors that arrived at the basolateral surface over the chase period. In contrast, receptors delivered directly to the apical plasma membrane were not proteolyzed by an exogenous protease (which is absent from the apical medium), but instead were efficiently cleaved by an endogenous apical plasma membrane protease to SC that was released into the apical medium. As SC comprises the major part of the radiolabeled pIgR, SC immunoprecipitated from the apical medium reflects the fraction of pIgR directly targeted to the apical surface. In all cases, 80–85% of the newly synthesized pIgR was chased to the cell surface (both apical and basolateral) at the end of the 90-min incubation. Thus, whenever a mutation caused a decrease in basolateral targeting, a proportional increase in apical delivery was detected. In addition, although expression levels varied from clone to clone over a two- to fourfold range, we found that the results described below did not vary significantly with expression levels.

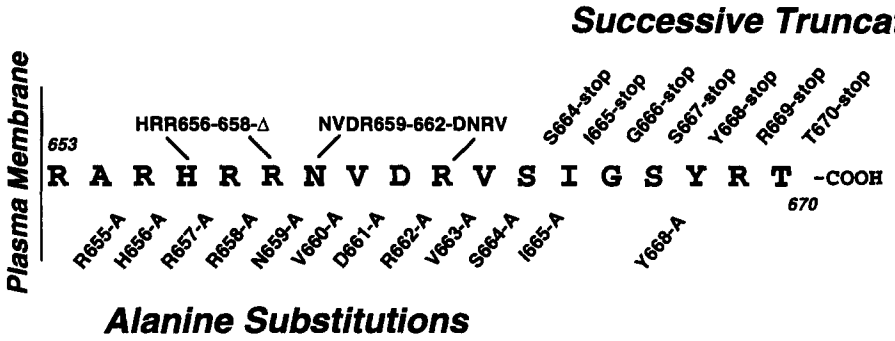

Figure 1. Mutagenesis of the 17-residue basolateral sorting signal. The cytoplasmic amino acids comprising the 17-residue basolateral sorting signal of the pIgR are depicted using the single letter code. Oligonucleotide-mediated mutagenesis was used to construct the mutant receptors. Single alanine substitutions (e.g., substitution of arginine at position 655 to alanine is designated: R655-A), deletion of the segment 656-HRR-658 (HRR656-658-Δ), and the mutant in which the sequence 659-NVDR-662 was shuffled to DNRV (NVDR659-662-DNRV) were all constructed in the context of the truncated T670-stop receptor. Truncation of residues was performed by mutating the codon that encodes for each of the indicated residues (e.g., threonine at position 670) to a stop codon (termed T670-stop).

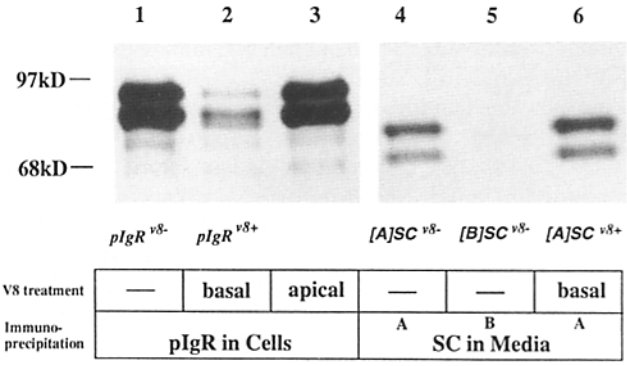

Figure 2. Determination of biosynthetic targeting to the basolateral cell surface by protease-based delivery assay. Filter-grown MDCK cells expressing the T670-stop mutant receptor were pulse labeled with [^{35}S]cys and chased in MEM/BSA in the absence of label and in the absence (lanes *1*, *4*, and *5*) or in the continuous presence of V8 protease in either the basal (lanes *2* and *6*) or the apical chamber (lane *3*). The pIgR was immunoprecipitated from cell lysates and soluble SC was immunoprecipitated from the apical (*A*) and basal (*B*) media. Immunoprecipitates were analyzed by SDS-PAGE and fluorography. The radioactivity levels of the relevant bands were determined by a PhosphorImager and designated as: $pIgR^{V8-}$; $pIgR^{V8+}$; $[A]SC^{V8-}$; $[B]SC^{V8-}$; $[A]SC^{V8+}$. Basolateral delivery percent is the fraction of radiolabeled pIgR proteolized by the basolaterally administered V8 protease. Apical delivery percent is the fraction of pIgR cleaved to SC at the apical surface and in the presence of basolateral V8 as indicated under Materials and Methods. In this case, basolateral delivery and apical delivery are 75 and 7%, respectively.

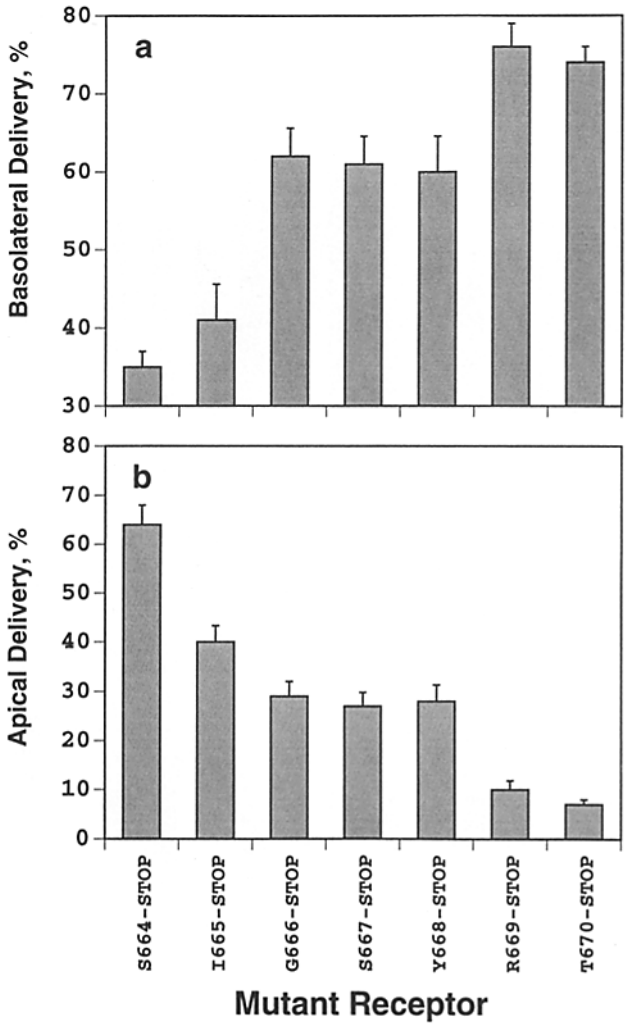

Figure 3. Delivery of truncated mutant receptors to the basolateral (*a*) and apical (*b*) surfaces of MDCK cells. MDCK cells expressing the various mutants were pulse-labeled with [^{35}S]cys and chased in the absence or in the continuous presence of V8 protease in the basolateral compartment as indicated in Materials and Methods and Fig. 2. Cell surface delivery of mutant receptors was quantitatively determined as described in Fig. 2 and under Materials and Methods. Measurements were performed on a pooled clone and on three different individual clones for each mutant. Results are mean ±SE of 10–13 determinations in each case.

Initially, we resolved individual residues involved in basolateral targeting, by systematically truncating the 17-mer segment from the COOH terminus (Fig. 3). Truncation at R669 (R669-stop) had no effect on basolateral targeting compared to the mutation T670-stop. Truncation at Y668 (Y668-stop) yielded a small but significant decrease in basolateral targeting (from 75 to ~60%) which was accompanied by a corresponding increase (from 6 to 25%) in apical cleavage of pIgR to SC. The greater sensitivity of apically released SC is due to the low baseline level of apical targeting (~6%) exhibited by the unimpaired mutant receptors. Truncations at residues S667 and G666 had no further effect compared to Y668-stop. Note that while almost all of the residues comprising the 17-mer signal are highly conserved across species, glycine at position 666 is not conserved; serine and arginine residues occupy the glycine position in rat and human pIgRs, respectively (Banting et al., 1989; Krajci et al., 1992). In addition, mutation of S667 to an alanine in the full-length pIgR had no effect on any of the receptor's phenotypes, including basolateral targeting (Casanova et al., 1990). Taken together, these data suggest that S667 and G666 are not essential for basolateral targeting of the pIgR. A further decrease in basolateral delivery was observed upon truncation at residues I665 or S664. Residues Y668, I665, and S664 are thus potentially implicated in basolateral sorting of the pIgR.

The functions of residues Y668, I665, and S664 were further examined by substituting each amino acid with an alanine in the context of the truncated T670-stop mutant. Alanine was chosen as it is less likely than other residues to impose electrostatic or steric effects, or to alter the main chain conformation (Cunningham and Wells, 1989). In contrast to the results obtained by the truncation studies, the results summarized in Fig. 4 show that the relatively conservative mutation I665-A or the less conservative change of S664-A had virtually no effect on basolateral delivery of the pIgR. In contrast, substituting Y668 for an alanine resulted in a relatively minor reduction in basolateral delivery, with values similar to those obtained for the truncated Y668-stop mutant. Therefore, a tyrosine at position 668 appears to be important for basolateral sorting, while the role of S664 and I665 remains unclear, as the Ala mutations and truncations yielded contradictory results.

To resolve this discrepancy we made individual internal deletions of S664 or I665. These were made in the context

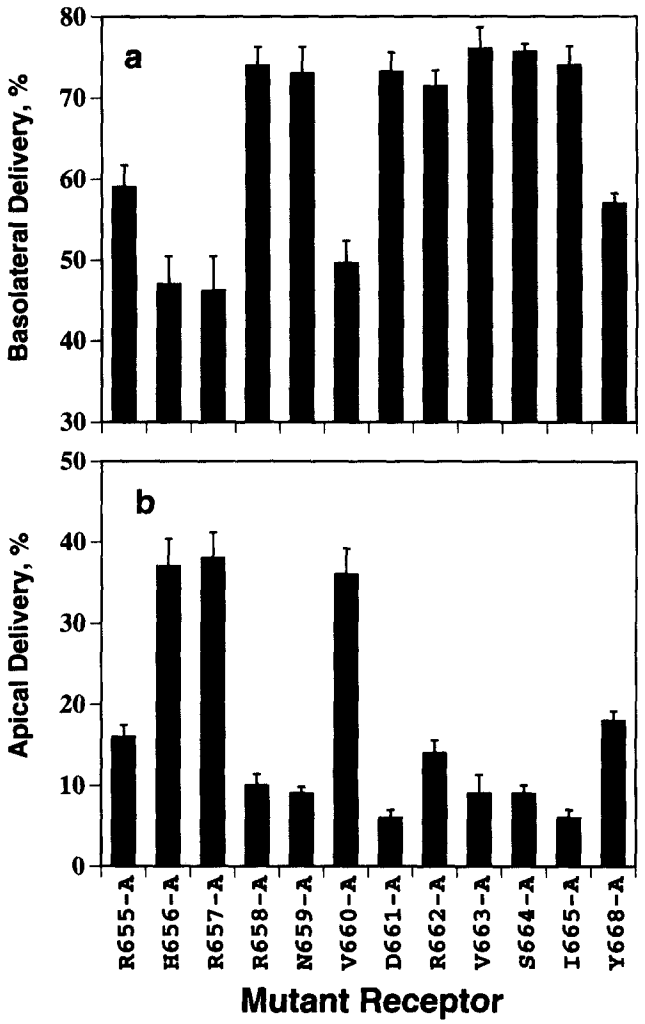

Figure 4. Delivery of single alanine substitution mutants to the basolateral (*a*) and apical (*b*) surfaces of MDCK cells. Quantitative determinations of receptor targeting to the cell surface were performed as described in Fig. 2 and under Materials and Methods. Measurements were performed on a pooled clone and on three different individual clones for each mutant. Results are mean ± SE of 10–13 determinations in each case.

of a pIgR with a full-length cytoplasmic tail, so as to minimize possible secondary effects due to conformational instability of shortened peptides or proximity of the negative charge contributed by the COOH terminus (see Discussion). Both of these mutants revealed efficient basolateral delivery with values comparable to the wild-type receptor (i.e., 80 ± 4% [mean ± S.E., n = 10] of the newly synthesized receptor is sorted directly from the TGN to the basolateral surface and 16 ± 1.5% is targeted to the apical surface). These data suggest that S664 and I665 are not essential for basolateral sorting.

We next constructed mutations that affected relatively large portions of the cytoplasmic domain in the region between R653 and V660. The positively charged cluster HRR656-658 was deleted in the context of the T670-stop template. The basolateral delivery of this mutant (designated HRR656-658-Δ) was significantly inhibited. About 45% of the mutant receptor was directed to the basolateral surface and 40% to the apical plasma membrane (data not shown). Similar results were obtained upon scrambling the sequence NVDR659-662 to DNRV659-662 (NVDR659-662-DNRV). This indicates that the order of residues between N659 and R662 is critical for basolateral targeting.

To define specific residues that mediate basolateral targeting in the region of R655-V663, we systematically replaced individual amino acids with an alanine. Residue R653, which abuts the transmembrane region, was not mutated as its positively charged side chain probably locks the transmembrane domain of the receptor in the lipid bilayer. R653 is followed by residue A654 in rabbit and human pIgRs (Banting et al., 1989; Krajci et al., 1992). The rat pIgR, however, has a valine residue at 654 (Banting et al., 1989), suggesting that this residue may not be essential for basolateral delivery. The results of the alanine-scanning mutagenesis (Fig. 4) demonstrate that substitutions of H656, R657, or V660 yield mutant receptors with non-polarized expression. Approximately equal amounts (40–45%) of the radiolabeled mutant receptors reached the apical and the basolateral surfaces. Similar data were obtained when mutations H656-A, R657-A, and V660-A were constructed in the context of the full-length wild-type tail (Aroeti, B., and K.E. Mostov, unpublished results). These results further support the involvement of those residues in basolateral targeting of the pIgR, and suggest that their sorting activity is not affected by the remainder of the cytoplasmic tail. They also imply that the effects that the indicated Ala substitutions had on the targeting of the T670-stop receptor are probably not due to conformational instability of the shorter tail.

Similar to Y668, substitution of R655 with an alanine yielded a smaller but significant effect on basolateral delivery, with only ~60% of the receptor targeted to the basal surface and 15–20% delivered apically (Fig. 4). In summary, our results suggest that H656, R657, and V660 are major determinants for basolateral targeting of the pIgR, whereas R655 and Y668 play a lesser, but yet significant role in the sorting process.

2D-NMR Secondary Structure Analysis of Synthetic Peptides Corresponding to Wild-type and Mutant 17-mer Basolateral Sorting Signals

We acquired two-dimensional proton NMR spectra of three synthetic 17 residue peptides in an attempt to characterize conformational features that might be relevant to pIgR basolateral targeting. One of these peptides (P-WT) corresponds to residues 653-669 of the pIgR, while the other two contain point mutations that were found to inhibit significantly basolateral targeting. For one of these peptides (P-R657A), alanine replaced arginine at the position corresponding to residue 657 of the receptor and for the other peptide (P-V660A), alanine replaced valine at the position corresponding to residue 660. The spectra were obtained at 5°C to stabilize as much as possible any ordered conformations and at pH 4.6 to minimize amide proton exchange with water. The relatively low pH introduces the possibility that the ionization state of H656 is not the same as found in vivo.

Proton resonance assignments for spin systems characterized by intra-residue through-bond connectivities were obtained from HOHAHA spectra (Bax et al., 1982). NOESY spectra (Wagner et al. 1981) were acquired to obtain sequential inter-residue through-space connectivities, that is $C^{\alpha}H_i$-

NH_{i+1}, $C^{\beta}H_i$-NH_{i+1} and NH_i-NH_{i+1} NOEs. Here, i and i+1 signify residues adjacent in sequence. Although arginine accounts for about one-third of the amino acid composition in each peptide, the resonances of the arginines were not completely degenerate and each arginine spin system was uniquely assigned. For example, in the P-WT NOESY spectrum, unique $C^{\alpha}H_i$-NH_{i+1} NOEs were found for the NH_2- and COOH-terminal arginines and two $C^{\alpha}H_i$-NH_{i+1} NOEs were readily identified for all tri-residue sequences containing an arginine as the middle residue, with the exceptions of H656-R657-R658 and R657-R658-N659. For these two arginines, the $C^{\alpha}H$ resonances are nearly degenerate so that the intra-residue $C^{\alpha}H$-NH cross peak of R658 overlaps the $C^{\alpha}H_i$-NH_{i+1} NOE of R657 and R658. However, unique $C^{\alpha}H_i$-NH_{i+1} NOEs were found for residues H656 and R657 and R658 and N659 in the NOESY spectrum of P-WT (and of P-V660A). Along with unambiguous $C^{\alpha}H_i$-NH_{i+1} NOEs found for sequential residue pairs, the assignments were confirmed in many cases by identification of $C^{\beta}H_i$-NH_{i+1} and NH_i-NH_{i+1} NOESY cross peaks. Fig. 5 shows the fingerprint and the NH-NH regions of the P-WT NOESY spectrum. Additional NOEs belonging to $C^{\alpha}H_i$-NH_{i+2} connectivities are also seen in the fingerprint region. The chemical shift assignments for P-V660A and PR657A are entirely consistent with each other and with those of P-WT. Assignment diagrams and summaries of all inter-residue NOEs for the three peptides are shown in Fig. 6.

While the strong $C^{\alpha}H_i$-NH_{i+1} NOEs found in the P-WT spectrum are typical of a peptide without ordered structure, the presence of NH_i-NH_{i+1} NOEs and medium range cross peaks (Fig. 5) indicates that P-WT also has a propensity to adopt ordered conformations that interconvert with disordered conformations. This interconversion must occur rapidly as only one complete set of resonances are found. For the following discussion, it is convenient to consider separately three segments of P-WT: residues R653-R658, residues R658-D661, and residues D661-R669.

There is considerable overlap of the $C^{\alpha}H$ and NH resonances for residues R655-N659 of P-WT (Fig. 5 *a*). This overlap precludes identification of NOEs indicative of ordered structure. With the exception of a relatively weak NH_i-NH_{i+1} NOE between H656 and R657 (Fig. 5 *b*), no other backbone–backbone cross peaks, associated with ordered structure, were identified. Thus, no correlation can be made between ordered conformations involving residues H656 and R657 of P-WT and the mutational studies that showed these two residues are important for proper basolateral targeting.

Beginning with the residue pair, R658/N659, NH_i-NH_{i+1} NOEs were identified for all subsequent pairs of residues except in one case where chemical shift degeneracy precluded identification (Fig. 6 *a*). Of these NOEs, the cross peak between residues V660/D661 is approximately twice as intense as all others, indicating closer average approach of those amide groups to each other. The identification of this NOE along with the weaker NH_i-NH_{i+1} NOE between N659/V660 and the presence of a $C^{\alpha}H_i$-NH_{i+2} NOE between N659 and D661 suggests that residues 658 to 661 have a significant tendency to adopt a β turn (Wüthrich et al., 1984; Dyson et al., 1988*a*). This turn is tentatively assigned as type I based on the relative intensities of the two NH_i-NH_{i+1} NOEs. The residue V660, shown by mutational studies to be important in basolateral targeting, would reside in position i+2 of such a turn.

A series of NH_i-NH_{i+1} NOEs, such as that found for residues 658 to 669, is characteristic of the so-called nascent helix (Dyson et al., 1988*b*). This type of structure was originally described for a peptide (derived from a helical region of myohemerythrin) as a conformational ensemble of turn-like structures and which upon addition of trifluoroethanol was stabilized as a helix with long-range order. Consecutive NH_i-NH_{i+1} NOEs are expected for helical structures, but neither $C^{\alpha}H_i$-NH_{i+3}, $C^{\alpha}H_i$-NH_{i+4}, nor $C^{\alpha}H_i$-$C^{\beta}H_{i+3}$ cross peaks diagnostic of a regular α- or 3_{10}-helix with long-range order were identified in the spectrum of P-WT. Further, the circular dichroism spectrum of P-WT, recorded in the presence of 33% (vol/vol) trifluorethanol at pH 4.6 and 5°C, was not characteristic of helix, showing only one minimum at 195 nm (spectrum not shown). Taken together, these observations suggest either that residues 658 to 669 are not part of a stable helix in the context of full-length pIgR or that other medium and long-range interactions, which are not adequately mimicked by trifluorethanol, are needed to stabilize helical structure between residues 658 to 669 of the pIgR. On the other hand, the presence of multiple $C^{\alpha}H_i$-NH_{i+2} NOEs between residues 658-669 in conjunction with the NH_i-NH_{i+1} NOEs is clear evidence for transitory turn-like structures in P-WT.

As mentioned above, besides the NOESY spectrum of P-WT, the spectra of two peptides derived from the sequences of mutant pIgR's were recorded. Comparison of NOESY spectra of peptides containing the endocytosis signal and mutated sequences for the LDLR, LAP, and the insulin receptor proved useful in correlating structure with function (Bansal and Gierasch, 1991; Eberle et al., 1991; Backer et al., 1992; Lehmann et al., 1992). As noted in the introduction, those studies correlated loss of a β-turn-like structure and function upon mutation. Replacement of R657 with alanine in P-R657A results in very little change in the NOESY spectrum (summarized in Fig. 6 *b*). Two additional NH_i-NH_{i+1} NOEs and an additional $C^{\alpha}H_i$-NH_{i+2} NOE between residues S667 and R669 were identified. But the NH_i-NH_{i+1} NOEs could not be found in the spectrum of P-WT due to resonance overlap. The weak C^{α}_i-NH_{i+2} NOE is also found in the spectrum of P-V660A (Fig. 6 *c*), indicating that it is not unique to the spectrum of P-R657A. Further, after normalizing the intensities of the NH_i-NH_{i+1} NOEs of P-WT and P-R657A to the N659 amide side chain exchange peak of each respective spectrum (data not shown), it was clear that no perturbation of identifiable conformations of P-WT occurs on substitution of an alanine at position 657. The normalized NH_i-NH_{i+1} NOE intensities are virtually the same in both spectra. Thus, alanine at position 657 does not disrupt structure distal to the substitution.

The NOESY spectrum of P-V660A is somewhat more informative than that of P-R657A. After normalizing the intensities of the NH_i-NH_{i+1} NOEs of P-WT and P-V660A in the manner described above, it was apparent that the relative intensity of the V660/D661 NOE decreases by approximately 50%, suggesting a destabilization in the putative β-turn-like conformation involving residues 658-661. Because of resonance overlap, it was impossible to determine if the $C^{\alpha}H_i$-NH_{i+2} cross peak of residues 659 and 661 is similarly affected. However, new cross peaks between $C^{\beta}H$ of A654

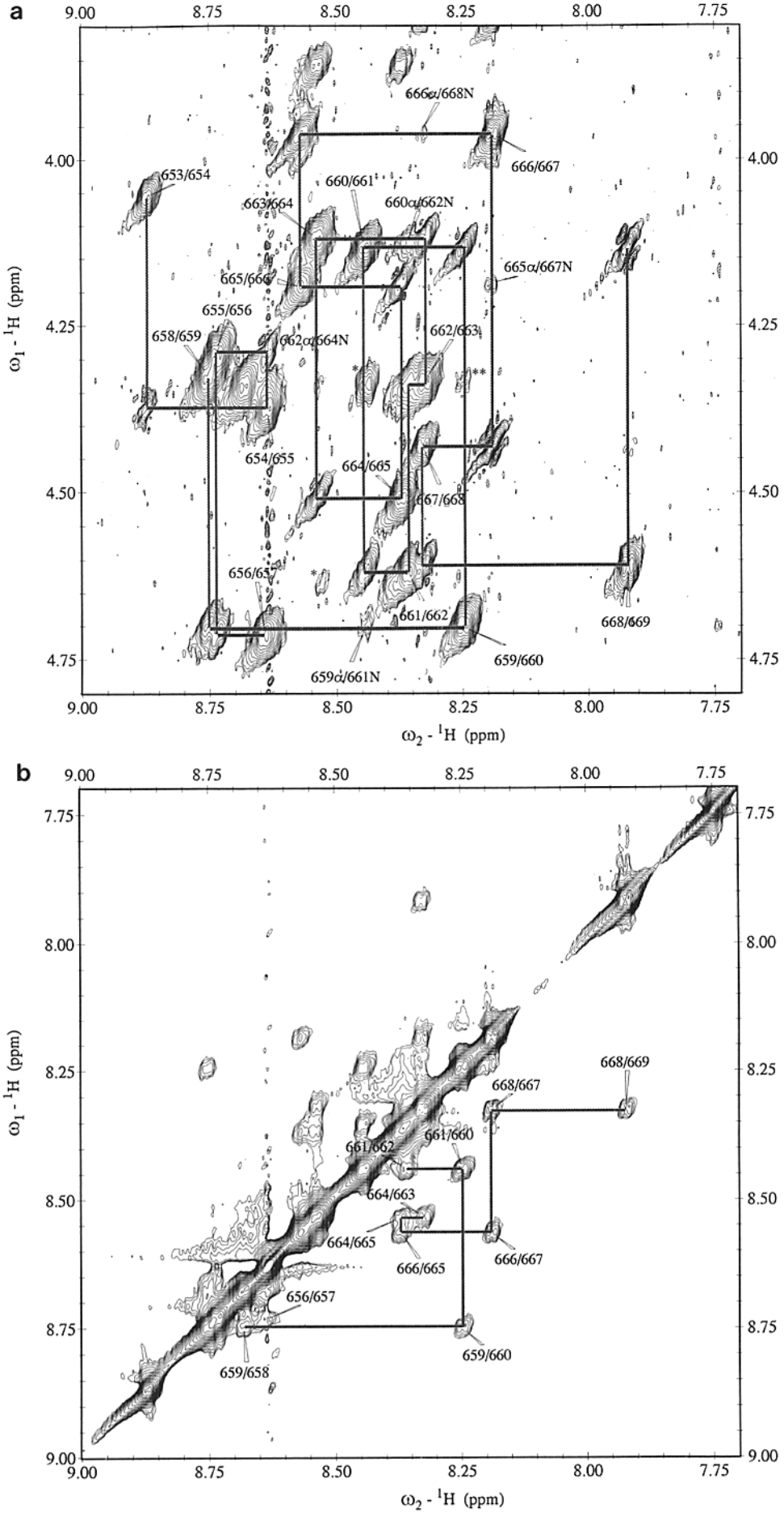

Figure 5. Portions of the 500 MHz spectrum of P-WT (pH 4.6, 5°C, 200 ms mixing time). (*a*) The fingerprint region. The connectivities between R653 to R657 and from R658 to R669 are traced out. Sequential $C^{\alpha}H_i$ – NH_{i+1} cross peaks are labeled with the appropriate residue numbers corresponding to those of the pIgR. Intra-residue $C^{\alpha}H_i$ – NH connecting sequential cross peaks are unlabeled. Also labeled are $C^{\alpha}H_i$ – NH_{i+2} cross peaks. The peaks labeled with an asterisk (*) could not be assigned. These cross peaks were not eliminated when the peptide was purified by cationic (Mono S) FPLC chromatography, followed by reverse phase chromatography suggesting that there is a second slowly interconverting conformer of P-WT present. The cross peak labeled with two asterisks (**) could not be unambiguously assigned and may be either an NOE between $C^{\alpha}H$ of R657 and NH of V660 or one between $C^{\alpha}H$ of R658 and NH of V660. (*b*) The NH – NH region. The connectivities between residues N659 to R662 and V663 to R669 are traced out. The labeling scheme is as above. This portion of the P-WT NOESY spectrum was contoured at a level twofold greater than that for the fingerprint region.

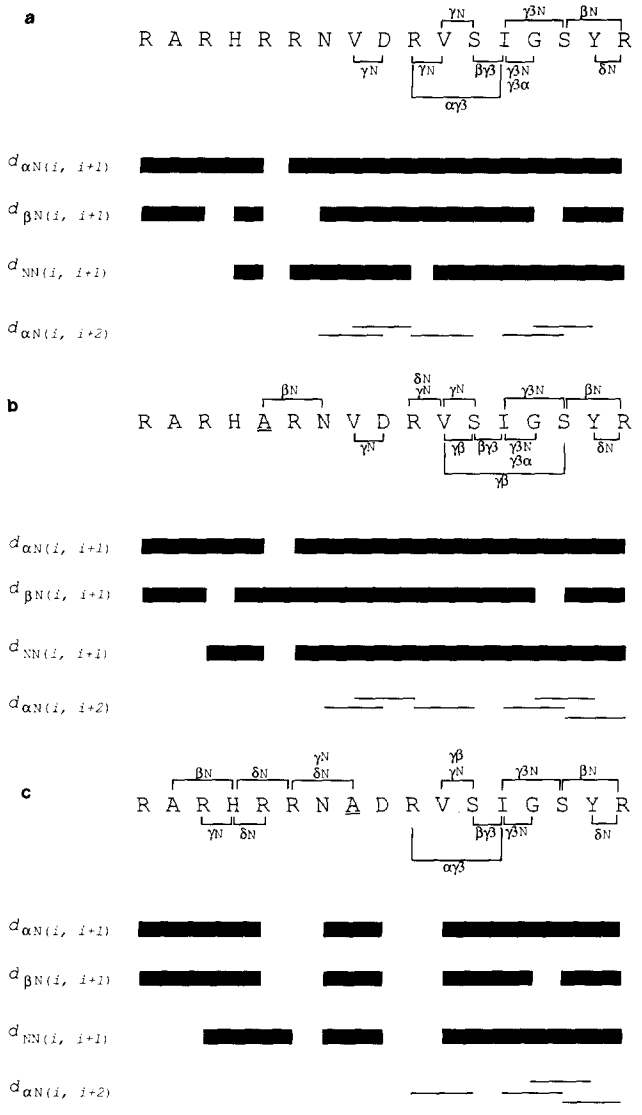

Figure 6. Sequential connectivity diagrams for: (*a*) P-WT; (*b*) P-R657A; and (*c*) P-V660A. The thicknesses of the lines do not indicate the strength of the NOE. Only the A654/R655 $NH_i - NH_{i+1}$ NOE is unambiguously absent in the spectra of all three peptides. Other sequential NOEs, not indicated in the diagrams, may be present but resonance overlap precluded positive identification. Additional side chain to backbone and side chain to side chain NOEs are indicated above and below the peptide sequence. For P-R657A and P-V660A the position of the amino acid substitution is marked by underlining the appropriate residue.

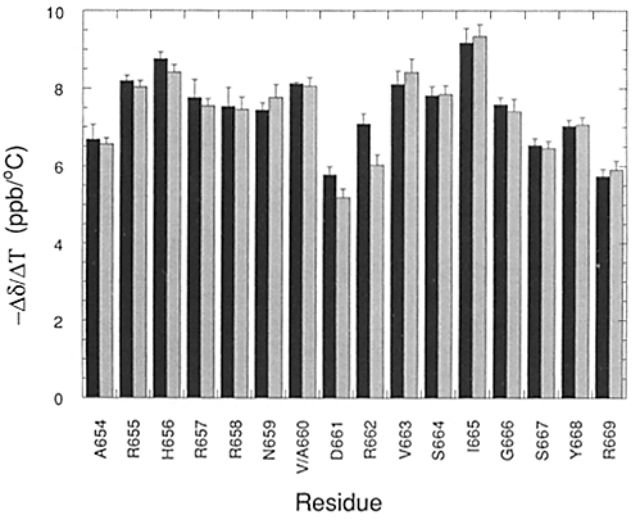

Figure 7. Correlation of amide proton chemical shift with temperature ($-\Delta\delta/\Delta T$). The chemical shifts of the amide backbone protons of P-Wt (■) and P-V660A (▨) were plotted versus temperature. The slope of the linear least squares fit for each amide proton data set is the temperature coefficient and is plotted here. The error bars are three standard errors of the slopes.

and NH of H656, $C^{\delta}H$ of H656 and NH of R658, and $C^{\beta}H$ and $C^{\gamma}H$ of R658 and NH of A660 were found (Fig. 6 *c*). The analogous cross peaks were absent from the spectra of P-WT and P-R657A. While the COOH-terminal nascent helix of P-V660A seemed to be unaffected, the appearance of the above mentioned NOEs suggests that the nascent helix propagates further toward the NH_2-terminal region when alanine substitutes for valine at position 660.

Additional evidence for a turn-like conformation involving residues 658 to 661 and possible disruption of that structure when V660 is replaced by alanine was obtained from a study of the temperature dependence of the amide chemical shifts for P-WT and P-V660A (Fig. 7). A decrease in the temperature coefficient ($-\Delta\delta/\Delta T$) of an amide proton resonance is usually taken as a measure of protection of that proton from exchange with solvent due to (intramolecular) hydrogen bonding (Dyson et al., 1988*a*). For P-WT, the amide of D661 appears to be most protected from solvent. This observation is consistent with others, outlined above, that D661 would occupy the i + 3 position of a β-turn, and its amide proton would therefore be expected to hydrogen bond with R658 in position i of the turn. However, contrary to expectations, the temperature coefficient of the amide proton of D661 in P-V660A, did not increase but rather decreased further. Also, the temperature coefficient of R662 decreased significantly. The observed decrease in the temperature coefficient of the amide proton of D661 may be due to an increased propensity of the side chain carboxyl to hydrogen bond with the backbone amide. Nonetheless, the significant changes in the temperature coefficients of D661 and R662 indicate local alterations in structure and are therefore consistent with a decrease in stability of the proposed turn involving residues R658-D661.

Discussion

Sequence Requirements for the Basolateral Sorting Signal

We have systematically examined the sequence requirements for the pIgR basolateral targeting signal and its possible secondary structure in solution using several mutational strategies and two-dimensional NMR spectroscopy. The results of these experiments are summarized in Fig. 8.

Progressive truncations from the COOH terminus of a pIgR containing only the 17-residue basolateral signal suggested that Y668, I665, and S664 may be important for basolateral sorting. Substitution of Y668 with Ala confirmed

Figure 8. Individual residues involved in basolateral targeting and possible secondary structure of the 17-residue basolateral sorting signal of the pIgR. The 17 cytoplasmic residues of the basolateral sorting signal of the pIgR is depicted. Based on the mutational analysis used in this study, the most important amino acids involved in polarized sorting of the pIgR to the basolateral surface of MDCK cells are indicated by a star. The less important residues are marked by a diamond. The residues shown by two-dimensional NMR to adopt a β-turn in solution are indicated by a black bar and the residues that tend to form a nascent helix are indicated by a cross-hatched bar.

that this residue plays a role in basolateral sorting. Previously we found that basolateral sorting was not affected upon mutating Y668 to Cys in the full-length pIgR (Okamoto et al., 1992). In contrast, as mentioned above alanine substitution of Y668 partially diminished basolateral targeting. It is possible that the Ala substitution at position 668 disrupted the basolateral sorting signal, whereas the Cys substitution did not. In addition, unlike the quantitative basolateral delivery assay applied in this study, the assay used to determine basolateral targeting of the mutant Y668 to Cys (Okamoto et al., 1992) was less quantitative and most likely not as sensitive in detecting small changes in basolateral targeting.

In contrast to the truncation results (Fig. 3), substitutions of I665 and S664 and Ala did not alter basolateral sorting, so the role of these residues was unclear. One possibility is that they are important, but the basolateral signal could tolerate an Ala at these positions. However, even though truncation of these residues had an effect on targeting, one cannot exclude the possibility that factors other than the truncated residues contributed to the altered phenotype. For example, at neutral pH the COOH-terminal carboxyl group bears a negative charge. Progressive truncation of residues from the COOH terminus changes the proximity of the charged moiety to possible sorting determinants residing in the non-truncated part of the tail. Consequently, the structure of the nontruncated region (and the sorting signal) might be disturbed. The negative charge may also interfere with interactions between the basolateral sorting machinery and a sorting signal possibly located in the non-truncated region. In both cases, a mutant receptor with impaired basolateral sorting activity might be observed even though the truncated residues are not part of the actual sorting signal.

To resolve the apparent contradiction between the Ala mutations and truncations at residues S664 and I665, we individually deleted these residues. We made these in the context of the full-length pIgR to avoid possible complications from moving the charged C-terminus too close to the putative signal. Also we reasoned that the structure of the signal in the context of the full-length tail might be more resistant to a non-specific destabilization due to removal of a residue. In both cases these deletions did not disrupt basolateral sorting. Unlike Ala mutations, internal deletions might be expected to have a high propensity to disrupt structure, even if the deleted residues are not truly part of the signal. The finding that the deletions of S664 or I665 did not alter basolateral sorting therefore can be taken as particularly strong evidence that these residues are not part of the basolateral signal. In conclusion, the preponderance of data (from Ala mutations and internal deletions) suggests that these residues are not part of the signal. The effects of truncations at these residues are most likely due to secondary effects of the truncations.

We then analyzed the region from 656 to 663, primarily by alanine scanning mutagenesis. The alanine mutations that yielded the largest in basolateral sorting were at H656, R657, and V660 (see Fig. 4), and we conclude that these residues are particularly important for basolateral sorting. Alanine mutations at R655 and Y668 had smaller effects on basolateral sorting (Fig. 4), suggesting that these residues play a lesser role in this process. Obviously, one should keep in mind that alanine scanning only examines the ability of these positions to tolerate this particular substitution. Nevertheless, alanine scanning is widely accepted as a useful approach to identify functionally important residues.

Basolateral targeting seems to be dependent on the positively charged segment RHR655-657. The importance of polar and charged residues has also been suggested in previous studies on internalization and basolateral targeting signals (Ktistakis et al., 1990; Trowbridge, 1991; Le Bivic et al., 1991; Matter et al., 1992). Interestingly, this positively charged cluster is located only two residues away from the transmembrane region of the molecule. In a previous study, the transferrin receptor internalization signal YXRF was shown to retain its activity only when separated by at least seven residues from the transmembrane region (Collawn et al., 1990). Our study suggests that the cytoplasmic residues RHR655-657 can be quite close to the plasma membrane and still mediate basolateral sorting of the pIgR.

Negatively charged phosphatidylserine molecules are concentrated in the cytoplasmic leaflet of the plasma membrane (Alberts et al., 1989), and presumably also in the Golgi. The juxtamembrane positively charged cytoplasmic residues may serve to shield the sorting determinant from this negatively charged surface and thereby facilitate sorting. Alternatively, the positively charged residues may directly interact with components of the basolateral sorting machinery. Recent observations proposed that heterotrimeric G_i proteins play a role in targeting from the TGN to the basolateral surface (Stow et al., 1991; Bomsel and Mostov, 1992; Pimplikar and Simons, 1993). This class of G proteins is known to be activated by positively charged peptides, such as the wasp venom mastoparan. An intriguing possibility is that the juxtamembrane basic residues of the basolateral sorting signal of the pIgR interact with a G_i protein.

Are there homologues of the pIgR basolateral targeting signal in other proteins? In a recent study, alignment of a 13-amino acid sequence implicated in basolateral sorting of the LDLR with the 17-mer sequence in the pIgR revealed five consensus residues: H/R819, S/N820, D822, T/S825, S828 in the LDLR aligned with residues R658, N659, D661, S664, S667 in the pIgR (Yokode et al., 1992). Residue V660, which functions in basolateral sorting of the pIgR, aligns with Q821 in the LDLR, pointing to a lack of residue conservation at the indicated position for these two receptors. However, to test the possibility that glutamine may still substitute for valine in the sorting determinant of the pIgR, we mutated V660 to glutamine in the context of the truncated T670-stop mutant. The mutant receptor V660-Q showed impaired

basolateral delivery with values similar to those observed for the mutant V660-A (basolateral delivery = 35 ± 5% and apical delivery = 48 ± 5% [mean ± S.E., n = 10]). Moreover, mutagenesis studies on the basolateral sorting signal of the LDLR demonstrated that three of the consensus residues are not required for basolateral targeting (Matter et al., 1992). Tyrosine 824, which is part of the distal basolateral sorting determinant of the LDLR, is not conserved; it is V663 in the pIgR. Taken together, these observations argue against the partial homology suggested between the distal basolateral signal of the LDLR and the basolateral signal of the pIgR.

In the case of the transferrin receptor the single cytoplasmic Tyr is important for endocytosis, but is not necessary for basolateral targeting (Hunziker et al., 1991; Dargemont et al., 1993). The cytoplasmic domain of the transferrin receptor also contains the sequence RQVD27-30, which resembles the tight-turn forming sequence RNVD658-661 in the basolateral signal of the pIgR. Interestingly, when a 36-cytoplasmic residue segment encompassing the RQVD sequence (and the Tyr-internalization signal) was deleted, a 20% reduction in the basolateral distribution of the transferrin receptor in MDCK cells was observed (Dargemont et al., 1993). It is therefore plausible that RQVD is part of a basolateral signal in the transferrin receptor.

Possible Structure of the Basolateral Sorting Signal

To obtain structural insights into the basolateral sorting signal, we studied the solution structures of P-WT, a peptide corresponding to the 17-residue basolateral sorting signal. Two-dimensional NMR spectroscopy suggested that a plausible ordered conformation of the peptide contains two structural motifs. The sequence RNVD658-661 tends to adopt a β-turn possibly of the type I conformation, whereas residues COOH-terminal to that turn contain a nascent helix structure which appear to be less stable than that of residues 658-661. Of the three crucial residues identified by the alanine scan, one residue (V660) is in position i+2 of the turn. The other two residues (H656 and R657) immediately precede the turn and are in a region for which ordered structure could not be identified. Tyrosine 668, which plays a lesser role in sorting, is located in the nascent helix. Arginine 655 precedes the turn, and as for H656 and R657, the structure in this region could not be determined.

As far as we know, this is the first structural data for a basolateral targeting signal that does not overlap with an endocytosis signal. Intriguingly we found that this signal, like endocytosis signals, contains an apparent β-turn. Our results raise the possibility that β-turns are a common feature of basolateral signals, including both those that do and do not overlap with endocytosis signals. The ability of a particular signal to function as a basolateral signal and/or endocytosis signal might then be determined by the presence and location of specific side-chains. In particular, endocytosis signals contain a Tyr (or other aromatic residue) at position i or i+3, whereas the β-turn in the basolateral signal of the pIgR lacks aromatic residues, but contains a bulky hydrophobic Val at position i+2.

The ordered conformations proposed here are low energy conformers for P-WT in solution and are thus the best available starting points for considering the in vivo structure of the sorting signal. However, several caveats must be considered. First, the peptide may assume a different conformation when anchored to the membrane via the membrane spanning segment. Indeed, Bansal and Gierasch reported that a peptide corresponding to the transmembrane domain and part of the cytoplasmic tail of the LDLR exhibited an enhanced stability of the nascent helix in the region of the tight-turn internalization signal (Bansal and Gierasch, 1991). Second, the 17-residue signal is ordinarily part of the 103-amino acid cytoplasmic domain of the pIgR and may have a different conformation in the context of the complete domain. However, the observation that this 17-residue segment can be functionally transplanted to a heterologous protein and can act as an autonomous basolateral targeting signal (Casanova et al., 1991) makes it more plausible that the structural characteristics of the peptide determined here are biologically relevant. Third, this signal is presumably recognized by another protein(s) that forms part of the sorting apparatus. Binding of this protein may alter the conformation of basolateral signal. In that case it will be extremely interesting to determine the bound conformation.

We also examined the effect of two Ala substitution mutations on the three-dimensional structure of the sorting signal peptide. For one of the mutations, R657-A, there was no detectable change in the β-turn and nascent helix regions of the peptide (Fig. 6 *b*). For technical reasons, the structural determination of the highly charged region (residues 653-657) of the peptide is less certain. If indeed there are no changes in the backbone structure of the signal, this might suggest that the side chain of the R657 is directly involved in recognition by a sorting molecule. In any case an important conclusion that can be drawn from these data is that the β-turn is not sufficient for basolateral sorting.

In contrast another mutation, V660-A, appears to destabilize the tight-turn but has no effect on the stability of the nascent helix conformation in the COOH-terminal region of the peptide, as shown by no significant alterations in the NH_i-NH_{i+1} NOE intensities (calculations not shown). This result is similar to observations by Bansal and Gierasch and others on mutations in endocytosis signals that appear to destabilize the β-turn, but differs in that the nascent helix is not also destabilized (Bansal and Gierasch, 1991; Backer et al., 1992; Lehmann et al., 1992). In these situations, one does not know if the mutation acts by altering the secondary structure and/or by changing a residue that is directly involved in recognition of the signal. Although more work may be necessary to determine if a β-turn is required for basolateral sorting, our data show that V660 is essential for both basolateral sorting and for the stability of the turn.

We thank G. Apodaca and C. Okamoto for critical reading of the manuscript and the members of the Mostov lab for helpful comments. K. Tang provided excellent technical assistance.

This research was supported by grants from National Institutes of Health RO1 AI 25144, a Cancer Research Institute Investigator Award, an Edward Mallinckrodt Foundation Scholarship, and a Charles Culpeper Foundation Scholarship to K. Mostov; a grant from the Lucille P. Markey Charitable Trust to the UCSF Program in Biological Sciences; and NIH grant GM39900 to F. Cohen. The UCSF Magnetic Resonance Laboratory was partially funded by NIH grant RR-01668 to I. D. Kuntz. B. Aroeti was the recipient of a Human Frontier Science Program Organization Fellowship and is currently supported by an American Heart Association California Affiliate Fellowship.

Received for publication 12 April 1993 and in revised form 14 September 1993.

References

Alberts, B., D. Bray, J. Lewis, M. Raff, K. Roberts, and J. Watson. 1989. Molecular Biology of the Cell (Second Edition). Garland Publishing Inc., New York. 281 pp.

Apodaca, G., B. Aroeti, K. Tang, and K. Mostov. 1993. Brefeldin A inhibits the delivery of the polymeric immunoglobulin receptor to the basolateral surface of MDCK cells. *J. Biol. Chem.* 268:20380–20385.

Backer, J. M., S. E. Shoelson, M. A. Weiss, Q. X. Hua, R. B. Cheatham, E. Haring, D. C. Cahill, and M. F. White. 1992. The insulin receptor juxtamembrane region contains two independent tyrosine/β-turn internalization signals. *J. Cell Biol.* 118:831–839.

Bansal, A., and L. M. Gierasch. 1991. The NPXY internalization signal of the LDL receptor adopts a reverse-turn conformation. *Cell.* 67:1195–1201.

Banting, G., B. Brake, P. Brathetta, J. P. Luzio, and K. K. Stanley. 1989. Intracellular targetting signals of polymeric immunoglobulin receptors are highly conserved between species. *FEBS (Fed. Eur. Biochem. Soc.) Lett.* 254:177–183.

Basus, V. J. 1984. Observation of 2D nuclear Overhauser effect crosspeaks involving amide protons in H_2O solutions of proteins. *J. Mag. Reson.* 60: 138–142.

Basus, V. J., M. Billeter, R. A. Love, R. M. Stroud, and I. D. Kuntz. 1988. Structural studies of α-bungarotoxin. 1. Sequence-specific ^{1}H NMR resonance assignments. *Biochemistry.* 27:2763–2771.

Bax, D. J., R. A. Haberkon, and D. J. Rubin. 1982. MLEV-17-based two-dimensional homonuclear magnetization transfer spectroscopy. *J. Mag. Reson.* 65:355–360.

Bomsel, M., and K. E. Mostov. 1991. Sorting of plasma membrane proteins in epithelial cells. *Curr. Opin. Cell. Biol.* 3:647–653.

Bomsel, M., and K. Mostov. 1992. Role of heterotrimeric G proteins in membrane traffic. *Mol. Biol. Cell.* 3:1317–1328.

Brietfeld, P. P., J. M. Harris, and K. M. Mostov. 1989*a*. Postendocytotic sorting of the ligand for the polymeric immunoglobulin receptor in Madin-Darby canine kidney cells. *J. Cell Biol.* 109:475–486.

Breitfeld, P., J. E. Casanova, J. M. Harris, N. E. Simister, and K. E. Mostov. 1989*b*. Expression and analysis of the polymeric immunoglobulin receptor. *Methods Cell Biol.* 32:329–337.

Brewer, C. B., and M. G. Roth. 1991. A single amino acid change in the cytoplasmic domain alters the polarized delivery of influenza virus hemagglutinin. *J. Cell Biol.* 114:413–421.

Caplan, M., and K. S. Matlin. 1989. Sorting of membrane and secretory proteins in polarized epithelial cells. *In* Functional Epithelial Cells in Culture. K. S. Matlin and J. D. Valentich, editors. Allan R. Liss, New York. 71–127.

Casanova, J. E., P. P. Breitfeld, S. A. Ross, and K. E. Mostov. 1990. Phosphorylation of the polymeric immunoglobulin receptor required for its efficient transcytosis. *Science (Wash. DC).* 248:742–745.

Casanova, J. E., G. Apodaca, and K. E. Mostov. 1991. An autonomous signal for basolateral sorting in the cytoplasmic domain of the polymeric immunoglobulin receptor. *Cell.* 66:65–75.

Collawn, J. F., M. Stangel, L. A. Kuhn, V. Esekogwu, S. Jing, I. S. Trowbridge, and J. A. Tainer. 1990. Transferrin receptor internalization sequence YXRF implicates a tight turn as the structural recognition motif for endocytosis. *Cell.* 63:1061–1072.

Cunningham, B. C., and J. A. Wells. 1989. High-resolution epitope mapping of hGH-receptor interactions by alanine scanning mutagenesis. *Science (Wash. DC).* 244:1081–1085.

Dargemont, C., A. Le Bivic, S. Rothenberger, B. Lacopetta, and C. K. Lukas. 1993. The internalization signal and the phosphorylation site of transferrin receptor are distinct from the main basolateral sorting information. *EMBO (Eur. Mol. Biol. Organ.) J.* 12:1713–1721.

Dyson, H. J., M. Rance, R. A. Houghten, R. A. Lerner, and P. E. Wright. 1988*a*. Folding of immunogenic peptide fragments of proteins in water solution. I. Sequence requirements for the formation of a reverse turn. *J. Mol. Biol.* 201:161–200.

Dyson, H. J., M. Rance, R. A. Houghten, P. E. Wright, and R. A. Lerner. 1988*b*. Folding of immunogenic peptide fragments of proteins in water solution. II. The nascent helix. *J. Mol. Biol.* 201:201–217.

Eberle, W., C. Sander, W. Klaus, B. Schmidt, K. von Figura, and C. Peters. 1991. The essential tyrosine of the internalization signal in lysosomal acid phosphatase is part of a β turn. *Cell.* 67:1203–1209.

Gersten, D. M., and J. J. Marchalonis. 1978. A rapid, novel method for the solid-phase derivatization of IgG antibodies for immune-affinity chromatography. *J. Immunol. Meth.* 24:305–309.

Gumbiner, B. 1990. Generation and maintenance of epithelial cell polarity. *Curr. Opin. Cell. Biol.* 2:881–887.

Hunziker, W., C. Harter, K. Matter, and I. Mellman. 1991. Basolateral sorting in MDCK cells requires a distinct cytoplasmic domain determinant. *Cell.* 66:907–920.

Krajci, P., D. Kvale, K. Tasken, and P. Brandtzaeg. 1992. Molecular cloning and exon-intron mapping of the gene encoding human transmembrane secretory component (the poly-Ig receptor). *Eur. J. Immunol.* 22:2309–2315.

Ktistakis, N. T., D. Thomas, and M. G. Roth. 1990. Characteristics of the tyrosine recognition signal for internalization of transmembrane surface glycoprotein. *J. Cell Biol.* 111:1393–1407.

Kunkel, T. A. 1985. Rapid and efficient site-specific mutagenesis without phenotypic selection. *Proc. Natl. Acad. Sci. USA.* 82:488–492.

Le Bivic, A., Y. Sambuy, K. Mostov, and E. Rodriguez-Boulan. 1990. Vectorial targeting of an endogenous apical membrane asialoglycoprotein and uvomorulin in MDCK cells. *J. Cell Biol.* 110:1533–1539.

Le Bivic, A., Y. Sambuy, N. Patzak, M. Patil, M. Chao, and E. Rodriguez-Boulan. 1991. An internal deletion in the cytoplasmic tail reverses the apical localization of human NGF receptor translated in MDCK cells. *J. Cell Biol.* 115:607–618.

Lehmann, L. E., W. Eberle, S. Krull, V. Prill, B. Schmidt, C. Sander, K. von Figura, and C. Peters. 1992. The internalization signal in the cytoplasmic tail of lysosomal acid phosphatase consists of the hexapeptide GPYRHV. *EMBO (Eur. Mol. Biol. Organ.) J.* 11:4391–4399.

Lisanti, M. P., and E. Rodriguez-Boulan. 1990. Glycophospholipid membrane anchoring provides clues to the mechanism of protein sorting in polarized epithelial cells. *Trends Biochem. Sci.* 15:113–118.

Maniatis, T., E. F. Fritsch, and J. Sambrook. 1982. Molecular Cloning: A Laboratory Manual. Cold Spring Harbor Laboratory, Cold Spring Harbor. 545 pp.

Matter, K., W. Hunziker, and I. Mellman. 1992. Basolateral sorting of LDL receptor in MDCK cells: the cytoplasm domain contains two tyrosine-dependent targeting determinants. *Cell.* 71:741–753.

Morris, G. A., and R. Freeman. 1978. Selective excitation in Fourier transform nuclear magnetic resonance. *J. Mag. Reson.* 29:433–462.

Mostov, K. E., A. de Bruyn Kops, and D. L. Deitcher. 1986. Deletion of the cytoplasmic domain of the polymeric immunoglobulin receptor prevents basolateral localization and endocytosis. *Cell.* 47:359–364.

Mostov, K. E., and N. E. Simister. 1985. Transcytosis. *Cell.* 43:389–390.

Mostov, K., G. Apodaca, B. Aroeti, and C. Okamoto. 1992. Plasma membrane protein sorting in polarized epithelial cells. *J. Cell Biol.* 116:577–583.

Nelson, W. J. 1992. Regulation of cell surface polarity from bacteria to mammals. *Science (Wash. DC).* 258:948–955.

Okamoto, C. T., S.-P. Shia, C. Bird, K. E. Mostov, and M. G. Roth. 1992. The cytoplasmic domain of the polymeric immunoglobulin receptor contains two internalization signals that are distinct from its basolateral sorting signal. *J. Biol. Chem.* 267:9925–9932.

Plateau, G. A., and M. Guéron. 1982. Exchangeable proton NMR without base-line distortion, using new strong-pulse sequences. *J. Am. Chem. Soc.* 104:7310–7311.

Pimplikar, S. W., and K. Simons. 1993. Apical transport in epithelial cells is regulated by a Gs class of heterotrimeric G protein. *Nature (Lond.).* 362:456–458.

Prill, V., L. Lehmann, V. K. Figura, and C. Peters. 1993. The cytoplasmic tail of lysosomal acid phosphatase contains overlapping but distinct signals for basolateral sorting and rapid internalization in polarized MDCK cells. *EMBO (Eur. Mol. Biol. Organ.) J.* 12:2181–2193.

Rodriguez-Boulan, E., and W. J. Nelson. 1989. Morphogenesis of the polarized epithelial cell phenotype. *Science (Wash. DC).* 245:718–725.

Rodriguez-Boulan, E., and S. K. Powell. 1992. Polarity of epithelial and neuronal cells. *Annu. Rev. Cell Biol.* 8:395–427.

Simons, K., and A. Wandinger-Ness. 1990. Polarized sorting in epithelia. *Cell.* 62:207–210.

States, D. J., R. A. Haberkorn, and D. J. Rubin. 1982. A two dimensional nuclear Overhauser experiment with pure absorption phase in four quadrants. *J. Mag. Reson.* 48:286–292.

Stow, J. L., J. B. de Almeida, N. Narula, E. J. Holtzman, L. Ercolani, and D. A. Ausiello. 1991. A heterotrimeric G protein, $G_{\alpha i-3}$, on Golgi membranes regulates the secretion of a heparan sulfate proteoglycan in LLC-PK_1 epithelial cells. *J. Cell Biol.* 114:1113–1124.

Thomas, D'N. C., B. Brewer, and M. G. Roth. 1993. Vesicular stomatitis virus glycoprotein contains a dominant basolateral sorting signal critically dependent upon a tyrosine. *J. Biol. Chem.* 268:3313–3320.

Trowbridge, I. S. 1991. Endocytosis and signals for internalization. *Curr. Opin. Cell Biol.* 3:634–641.

Urban, J., K. Parczyk, A. Leutz, M. Kayne, and C. Kondor-Koch. 1987. Constitutive apical secretion of an 80-kD sulfated glycoprotein complex in the polarized epithelial Madin-Darby canine kidney cell line. *J. Cell Biol.* 105:2735–2743.

Vaux, D. 1992. The structure of an endocytosis signal. *Trends Cell Biol.* 2:189–192.

Wagner, G., A. Kumar, and K. Wüthrich. 1981. Systematic application of two-dimensional ^{1}H nuclear-magnetic-resonance techniques for studies of proteins. *Eur. J. Biochem.* 114:375–384.

Wüthrich, K., M. Billeter, and W. Braun. 1984. Polypeptide secondary structure determination by nuclear magnetic resonance observation of short proton-proton distances. *J. Mol. Biol.* 180:715–740.

Yokode, M., R. K. Pathak, R. E. Hammer, M. S. Brown, J. L. Goldstein, and R. G. W. Anderson. 1992. Cytoplasmic sequence required for basolateral targeting of LDL receptor in livers of transgenic mice. *J. Cell Biol.* 117:39–46.